polysaccharides

MDPI

Article

Layer-by-Layer Assembling and Capsule Formation of Polysaccharide-Based Polyelectrolytes Studied by Whispering Gallery Mode Experiments and Confocal Laser Scanning Microscopy

Stefan Wagner [1,2], Mateusz Olszyna [1], Algi Domac [1], Thomas Heinze [2,†], Martin Gericke [2,*,†] and Lars Dähne [1,*]

[1] Surflay Nanotec GmbH, D-12489 Berlin, Germany; s.wagner@surflay.com (S.W.); m.olszyna@surflay.com (M.O.); a.domac@surflay.com (A.D.)
[2] Centre of Excellence for Polysaccharide Research, Institute of Organic Chemistry and Macromolecular Chemistry, Friedrich Schiller University of Jena, Humboldtstraße 10, D-07743 Jena, Germany; thomas.heinze@uni-jena.de
* Correspondence: martin.gericke@uni-jena.de (M.G.); l.daehne@surflay.com (L.D.)
† Members of the European Polysaccharide Network of Excellence (EPNOE); http://www.epnoe.eu (accessed on 10 June 2024).

Abstract: The layer-by-layer (LbL) assembling of oppositely charged polyelectrolytes was studied using semi-synthetic polysaccharide derivatives, namely the polycations 6-aminoethylamino-6-deoxy cellulose (ADC) and cellulose (2-(ethylamino)ethylcarbamate (CAEC), as well as the polyanion cellulose sulfate (CS). The synthetic polymers poly(allylamine) (PAH) and poly(styrene sulfonate) (PSS) were employed as well for comparison. The stepwise adsorption process was monitored by whispering gallery mode (WGM) experiments and zeta-potential measurements. Distinct differences between synthetic- and polysaccharide-based assemblies were observed in terms of the quantitative adsorption of mass and adsorption kinetics. The LbL-approach was used to prepare µm-sized capsules with the aid of porous and non-porous silica particle templates. The polysaccharide-based capsule showed a switchable permeability that was not observed for the synthetic polymer materials. At ambient pH values of 7, low-molecular dyes could penetrate the capsule wall while no permeation occurred at elevated pH values of 8. Finally, the preparation of protein-loaded LbL-capsules was studied using the combination of CAEC and CS. It was shown that high amounts of protein (streptavidin and ovomucoid) can be encapsulated and that no leaking or disintegration of the cargo macromolecules occurred during the preparation step. Based on this work, potential use in biomedical areas can be concluded, such as the encapsulation of bioactive compounds (e.g., pharmaceutical compounds, antibodies) for drug delivery or sensing purposes.

Keywords: polysaccharides; polyelectrolytes; layer-by-layer assembling; whispering gallery mode; capsules; protein encapsulation

check for updates

Citation: Wagner, S.; Olszyna, M.; Domac, A.; Heinze, T.; Gericke, M.; Dähne, L. Layer-by-Layer Assembling and Capsule Formation of Polysaccharide-Based Polyelectrolytes Studied by Whispering Gallery Mode Experiments and Confocal Laser Scanning Microscopy. *Polysaccharides* **2024**, *5*, 422–434. https://doi.org/10.3390/polysaccharides5030026

Academic Editor: Paschalis Alexandridis

Received: 11 June 2024
Revised: 12 July 2024
Accepted: 1 August 2024
Published: 14 August 2024

Copyright: © 2024 by the authors. Licensee MDPI, Basel, Switzerland. This article is an open access article distributed under the terms and conditions of the Creative Commons Attribution (CC BY) license (https://creativecommons.org/licenses/by/4.0/).

1. Introduction

Layer-by-layer (LbL) assembling has become a highly versatile and attractive approach for the surface functionalization, encapsulation, and immobilization of biomolecules with promising prospects across various fields [1]. The LbL-process, first described in 1991, is based on the self-limited alternating adsorption of oppositely charged polymers (polyelectrolytes) from aqueous solutions onto almost every type of surfaces [2,3]. This leads to homogeneous multilayer films with a thickness for each layer in the nanometer range [4,5]. Transferring the planar LbL-process to colloidal systems allowed for the preparation of hollow capsules obtained after dissolution of the core material [6]. The semi-permeability of the LbL-films of capsules makes them promising delivery tools for therapeutic drugs and

bioactive macromolecules [3,7,8]. Despite the potential of LbL-assemblies, their transfer into medical applications has been held back by challenges, particularly regarding the cytotoxicity associated with commonly employed synthetic polymers (in particular, cationic ones). The mostly studied LbL-materials employ combinations of poly(allylamine) (PAH) or poly(diallyldimethylammonium chloride) as polycations and poly(styrene sulfonate) (PSS) or poly(methacrylic acid) as polyanions [9,10].

In the ongoing quest for safer alternatives, polysaccharides have gained attention as a promising class of polymers for medical applications. These biopolymers have distinct advantages over synthetic polymers when it comes to developing biomaterials and it is possible to chemically modify polysaccharides to further fine-tune their properties and introduce new functionalities, such as ionic moieties [11]. Anionic polysaccharides and polysaccharide derivatives, such as alginate, carrageenan, carboxymethyl cellulose, and cellulose sulfate (CS), have been explored in the context of LbL-materials and have proved to exhibit desirable properties for biomedical applications [10,12]. Nevertheless, the exploration of cationic polysaccharides, which are necessary for establishing charge reversal interactions within LbL-assemblies, has been restrained, with chitosan representing the most extensively investigated polysaccharide-based polycation to date [5].

Chitosan is a natural product derived by the deacetylation of chitin found in crustaceans and has been used as a cationic polyelectrolyte in many LbL-studies, mainly for the encapsulation of active compounds [13]. Despite its promising features, the reproducible application of chitosan is somewhat hampered. The degree of deacetylation of available chitosan that varies greatly between 70 and 90 % for different batches dictates the charge density varies and, as such, the whole LbL-assembling process [14,15]. Moreover, chitosan has a rather low pK_A value (around 6.4) because the secondary amino group is directly attached to the polymer backbone [16]. The polymer is mostly deprotonated at pH values above 6, which results in poor water solubility and weaker electrostatic interaction in the LbL-assemblies [17,18]. Consequently, there is a strong demand to diversify the repertoire of cationic as well as anionic polysaccharide-based polyelectrolytes that are suitable for LbL-applications, biocompatible coatings, and encapsulation strategies [19–26].

The chemical derivatization of cellulose and other polysaccharides enables the synthesis of functional biobased polymers with tailored physical, chemical, and biological properties. "Aminocelluloses" are a class of structurally diverse cellulose derivatives that contain one or more substituents with a primary, secondary, or tertiary amino moiety [27]. They received great interest because they are able to adsorb onto the surface of different types of materials and because they are able to act as polyanions for potential LbL-assembling. Moreover, it was shown that aminocelluloses are biocompatible and can feature bioactive properties (e.g., antimicrobial activity) [28,29]. Aminocelluloses are well soluble in water at low and high pH values. The synthesis of these compounds can be achieved by two different approaches. Tosylated cellulose reacts with different types of di- and trifunctional amines under nucleophilic displacement reactions [30]. Cellulose phenyl carbonates can be converted with various types of amines that contain either primary (require protecting groups), secondary, or tertiary amino groups, as well as quaternary ammonium groups, to yield the corresponding functional cellulose carbamates [31,32]. Both synthesis routes are straightforward and offer a broad structural diversity in terms of the amino moieties that can be introduced. CS is an anionic cellulose derivative that is very promising in the context of LbL-assemblies because (a) it has been used with great success as the polyanion component and (b) it also shows pronounced bioactivity and biocompatibility [33–35].

Several semisynthetic polyelectrolytes, e.g., those derived by the chemical modification of chitosan, dextran, and marine polysaccharides, have been described recently in the context of LbL-assemblies [12,36–38]. Following the advances in homogeneous cellulose chemistry, the focus of the present work was on cellulose derivatives with cationic amino groups (aminocellulose) or anionic sulfate groups (cellulose sulfates) as polyelectrolytes [32,33,39]. These compounds are easily accessible by the chemical derivatization of cellulose using

recently described synthesis approaches. Previous studies usually focus on the characterization of two-dimensional assemblies on planar surface substrates by procedures such as dipping and spin-coating, which potentially enables the use of established analytical methods such as IR- and UV-Vis spectroscopy as well as atomic force microscopy [25,26,36]. The focus of the present work was placed on the three-dimensional particles and capsules with rather thin polyelectrolyte layers due to their practical relevance (e.g., for the encapsulation of proteins), which required alternative analytical tools. Thus, whispering gallery mode (WGM) experiments were employed for the first time to gain comprehensive insight into the kinetics of the LbL-assembling of spherical particles. Furthermore, the preparation of LbL-capsules as well as the encapsulation of proteins was studied by confocal laser scanning microscopy (CLSM) experiments.

2. Materials and Methods

2.1. Materials

Poly(allylamine) (PAH; hydrochloride, molecular weight: 40,000 g/mol) was obtained from Beckmann-Kenko (Bassum, Germany). Poly(styrene sulfonate) (PSS; sodium salt, molecular weight: 70,000 g/mol) and all other chemicals were purchased from Sigma Aldrich (Taufkirchen, Germany). Polystyrene (PS) particles (diameter: 10 µm) were provided by Surflay GmbH (Berlin, Germany). Solid silica particles (diameter: 4.3 µm) were obtained from microParticles GmbH (Berlin, Germany) and porous silica beads (diameter: 5 µm, pore widths: 12 nm) were provided by Silicycle Inc. (Québec, QC, Canada). Cellulose sulfate (CS; sodium salt, degree of substitution/DS: 1.14), 6-aminoethylamino-6-deoxy cellulose (ADC; DS: 0.64), and cellulose (2-(ethylamino)ethylcarbamate (CAEC; DS: 1.57) were prepared by homogeneous derivatization of cellulose as previously described in the literature [32,33,39].

2.2. Methods and Measurements

The zeta-potential of PS sensor particles was recorded after each coating step using a Nanosizer LS (Malvern Panalytical/Worcestershire, UK) under standard condition of 10 mM Tris-buffer at pH value of 7. A confocal laser scanning microscope (CLSM; TCS-SPE, Leica Microsystems GmbH, Wetzlar, Germany) with a 63× objective was employed. For visualization and quantification of the fluorescence intensity, the settings were adjusted for the rhodamine tags (Rho; excitation: 532 nm, intensity: 33 %, emission detection: 545–625 nm) and 4-chloro-7-nitrobenzo-2-oxa-1,3-diazole (NBD-Cl; excitation: 405 nm, intensity: 15 %, emission detection: 500–600 nm) and the photomultiplier voltage was adjusted accordingly. For visualization of polymers containing amino groups, the capsules were incubated with an excess of NBD-Cl for 1 h and washed with water afterwards.

2.2.1. Evaluation of the Polyelectrolyte Layer-by-Layer (LbL) Assembling by Means of Whispering Gallery Mode (WGM) Experiments

Coating solutions were prepared in buffered solution (0.2 M sodium chloride, 50 mM sodium acetate, pH value adjusted to 5.6) with a mass concentration of 1 g/L polyelectrolyte. LbL-coating was performed by incubating the substrates (10 mg/1 mL of PS particles) in excess polyelectrolyte solution (1 mL) for 20 min at room temperature followed by three washing steps with water to remove non-adsorbed polymer. The subsequent layers were applied in the same way using a polyelectrolyte with opposite charge (stack of two layers, bilayer). The coating experiments were started by applying two bilayers of PSS/PAH followed by one layer of PSS onto the PS particles. Afterwards, the experiments were started by applying the polycations first.

The LbL-coating of PS particles was studied on a WhisperSense device (Surflay GmbH, Berlin, Germany) by means of WGM experiments. A microfluidic chip with prefabricated trapping holes array (20 × 50 microwells, in diameter of 12 µm; supplied by Stratec Biomedical AG/Birkenfeld, Germany) was loaded with precoated 10 µm PS sensor particles (two PSS/PAH bilayers and one PSS layer) and rinsed with running buffer (0.2 M sodium

chloride, 50 mM sodium acetate, pH value adjusted to 5.6) at a flowrate of 80 µL/min (4.6 mm/s).

For analyzing the kinetics of polyelectrolyte adsorption, coating solutions were pumped through the chip (80 µL/min) and the kinetics and quantity of adsorption were recorded. The chips were rinsed with running buffer (0.2 M sodium chloride, 50 mM sodium acetate, pH value adjusted to 5.6) after each coating step to remove any unspecific bounded polyelectrolytes before the next coating step with an oppositely charged polymer was performed. The real-time monitoring of adsorbed layers was continued until four double layers were reached. For quantitative evaluation of the polyelectrolyte binding, ten WGM sensors were measured before and after addition of each polyelectrolyte type. After the assembling of LbL-films, the WGM sensors were washed by borate buffer (pH value of 10) in order to test the stability of the coating at high pH values.

Each LbL-assembling experiment was performed in triplicates. The data were analyzed with WhisperSense software (V 1.1.2)and the adsorbed mass (area density mg/m^2) of polyelectrolytes was calculated using the formula proposed by Himmelhaus et al. [40]:

$$\Delta\lambda_m = \lambda_m \frac{\Delta R}{R} \qquad \sigma = \frac{\rho}{3} \frac{(R + \Delta R)^3 - R^3}{R^2} \tag{1}$$

λ: peak position (520 nm); $\Delta\lambda_m$: peak shift; m: mode number; R: particle radius; σ: surface mass density; ρ = mass density of the adsorbate (1.35 g/cm^3).

2.2.2. Preparation of LbL-Microcapsules

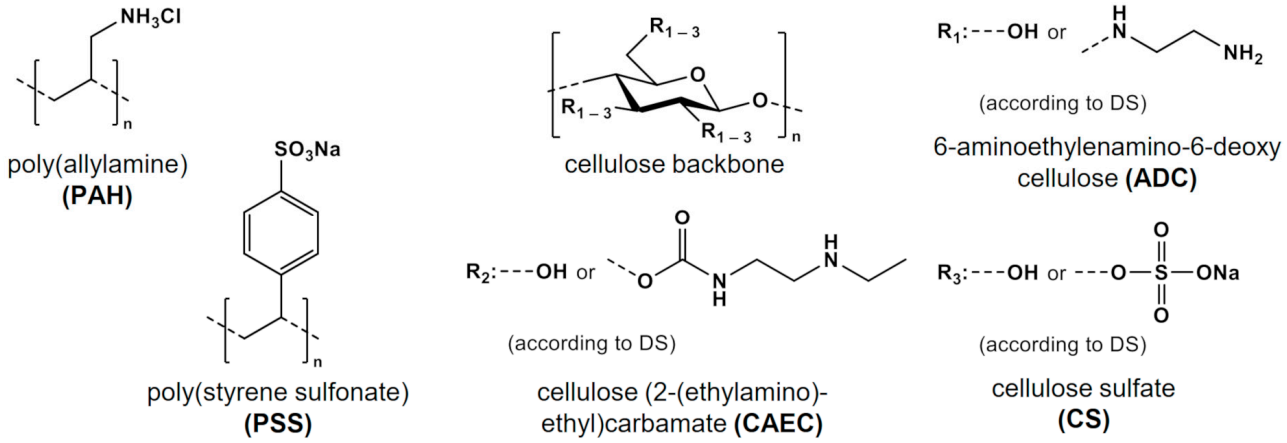
Microcapsules were prepared by adapting a patented procedure that was developed previously [41]. In short, hollow capsules were produced by starting with solid silica particles that were coated with one layer of CAEC followed by three bilayers of CS/CAEC. For protein-loaded capsules, Rho-labeled proteins (streptavidin–Rho or ovomucoid–Rho; manufactured by Surflay GmbH, Berlin, Germany) were loaded into spherical silica beads at a pH value of 7.4 (PBS buffer) and coated with three bilayers of CS/CAEC. In both cases, the silica core was removed by immersing the LbL-covered particles (0.5 mL, 0.1 wt.% particles) in dissolution buffer (0.5 mL) containing 2 g/L CS, 0.5 M ammonium acetate, and 0.5 M ammonium hydrogen difluoride at a pH value of 7.0 (adjusted with aqueous NH_3). After dissolution of the silica core, the protein capsules were washed extensively with water.

3. Results and Discussion

The layer-by-layer (LbL) assembling of polysaccharide-based polyelectrolytes was studied using two different polycations, namely aminoethylamino-6-deoxy cellulose (ADC) and cellulose (2-(ethylamino)ethylcarbamate (CAEC), and one polyanion, namely cellulose sulfate (CS; Scheme 1). These compounds are easily accessible by the chemical derivatization of native cellulose and were chosen due to their potential biocompatibility and/or bioactivity [28,29,34,35]. For comparison, the synthetic polyelectrolytes poly(allylamine) (PAH) and poly(styrene sulfonate) (PSS) were included in this study. In a first set of experiments, the stepwise assembling of the different polyelectrolytes into LbL-films was studied by means of whispering gallery mode (WGM) experiments. Afterwards, the preparation and protein loading of LbL-capsules was investigated. LbL-assembling is predominately based on strong electrostatic interactions but minor contributions from other non-covalent interactions (hydrogen bonding, van der Waals interaction) can also play a role.

A WhisperSens biosensing platform was employed to investigate the stepwise LbL-assembling of different types of polyelectrolytes, starting with the polycations. Three combinations of polyelectrolyte were tested: ADC/CS, CAEC/CS, and the LbL-standard combination PAH/PSS as reference. To create a negatively charged surface, the poly(styrene)-based WGM particles were coated with PSS through an electrostatic interaction followed by two double layers of PAH and PSS. A stepwise increase in the WGM shifts was observed for each adsorption step, which was due to the adsorption of polymers on the surface (Figure 1).

The direct comparison showed that the increase in WGM shift was most pronounced for the adsorption of PAH/PSS, followed by ADC/CS and CAEC/CS (Figure 1b). The adsorbed masses and molar amounts, which were calculated from the WGM shifts, showed a similar trend. After depositing four bilayers, the buffer system was changed from a washing buffer (50 mM sodium acetate, pH value of 5.6) to a more basic buffer (50 mM bortate, pH value of 10.0) to evaluate the stability of the LbL-assemblies at very high pH values. Due to the different refractive index of this buffer, it was changed back to the washing buffer in order to evaluate the desorbed amount. The combination of PAH/PSS was the most stable one and showed only a small absolute decrease in WGM shift. For the polysaccharide-based polyelectrolytes, a stronger decrease was observed, which can be attributed to a partial desorption or dissolution of the polyelectrolytes. However, it can be speculated that only the outer double layer is affected because the WGM shifts decreased to a similar level to that obtained after the third double layer attachment. Moreover, the decrease was much stronger for the system using ADC although the initial amount of adsorbed polymer was higher. The reason for the desorption is probably a deprotonation of the primary (ADC) and secondary amino groups (CAEC). For fully protonated polycations, the charge density for PAH (16.9 mmol/g) is higher compared to ADC (6.8 mmol/g) and CAEC (4.6 mmol/g), which explains the higher stability of the PAH/PSS combination. When comparing the two cellulose-based polycations, CAEC possesses a secondary amino group, which has a higher pK_A value that contributes to a higher degree of protonation, i.e., higher stability.



Scheme 1. Molecular structures of polycations and polyanions used in this study.

The WGM experiments on the LbL-assembling of PAH/PSS films confirmed previous findings obtained from quartz crystal microbalance (QCM) and ellipsometry experiments [42]. These have shown a classical linear increase in the LbL-film with a larger shift for the polyanion layer (PSS) than for the polycation (PAH). This was also observed in the present work (Figure 1a). However, the molar ratio between the monomer units shows a slight excess of the polycation due to the higher molecular weight of the PSS monomer unit and probably incomplete protonation of the primary amino groups of PAH. In the case of polysaccharide-based combinations ADC/CS and CAEC/CS (Figure 1c), the LbL-film showed an explicit exponential growth regime, which indicates that the adsorbed mass of polyelectrolytes increased significantly for each subsequent layer [43]. It is worth noting that the amount of polyelectrolyte per unit of sensor area ($\mu mol/m^2$) is higher for PAH/PSS when compared to ADC/CS and even more pronounced when compared to CAEC/CS. This indicates a lower affinity between the polysaccharide-based polyelectrolytes, probably due to the differences in charge density.

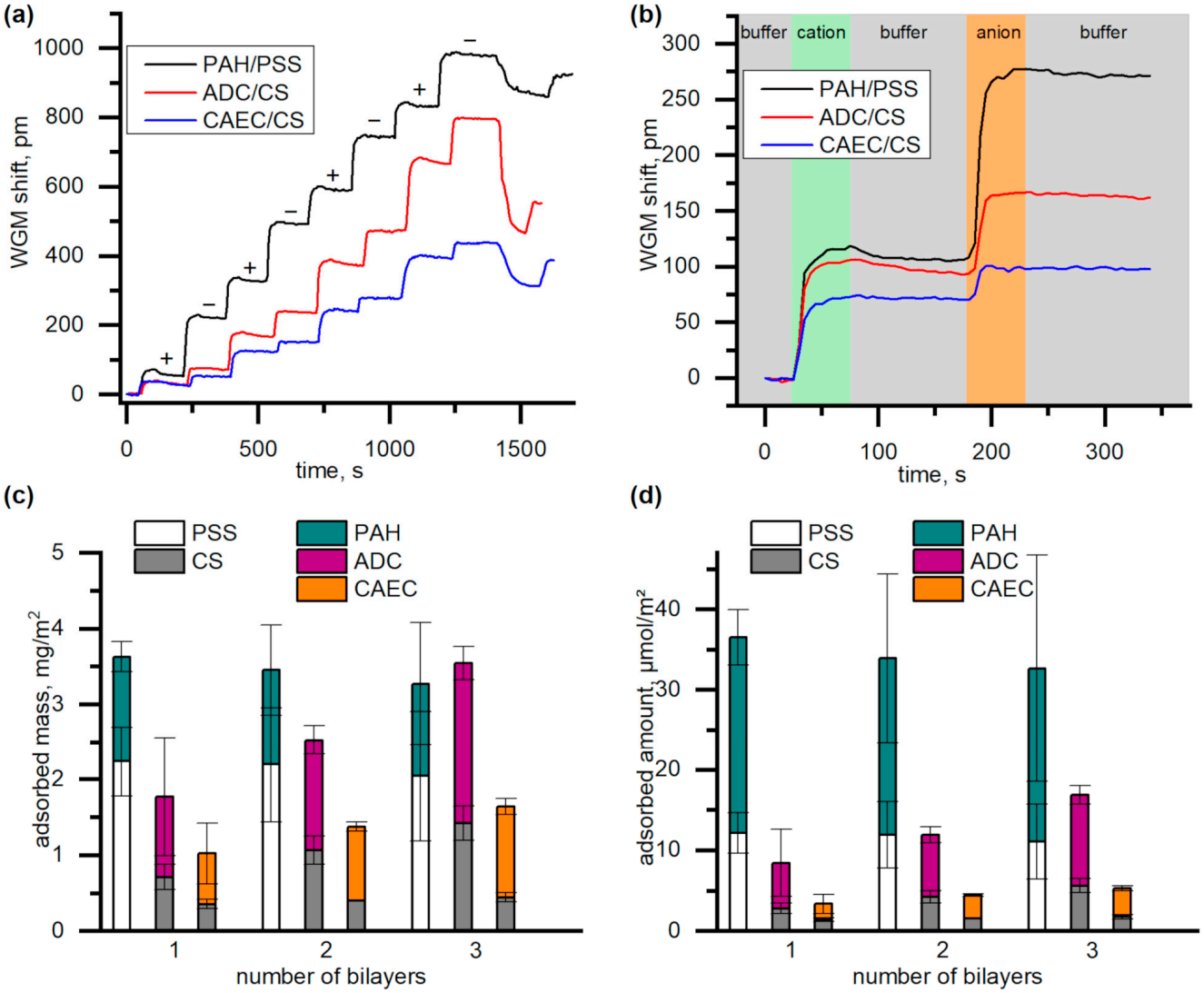


Figure 1. Results of whispering gallery mode adsorption experiments for the layer-by-layer assembling of bilayers of polycations (PAH: poly(allylamine); ADC: aminoethylamino-6-deoxy cellulose; CAEC: cellulose (2-(ethylamino)ethyl)carbamate) and polyanions (PSS: poly(styrene sulfonate); CS: cellulose sulfate) followed by a stability test against borate buffer (50 mM, pH value of 10) and PBS buffer displayed (**a**) over the whole process and (**b**) zoomed in for the second bilayer adsorption (after normalization to t = 0 s and WGM shift = 0 pm). Results for the quantification of the adsorption in terms of (**c**) mass of polyelectrolytes and (**d**) amount of polymer repeating units.

The kinetics of the adsorption for all three systems were compared in detail (Figure 2). At a high mass concentration of 1 g/L, similar behavior was observed in all cases. In order to evaluate the affinity of the coating polyelectrolyte to the complementary polyelectrolyte surface, the adsorption of the polycation was studied at a lower mass concentration of 0.1 g/L. For the synthetic polymers, a similar behavior was observed compared to the previous experiments, and the quantitative differences were small. For the assembling of an ADC/CS-bilayer, the slope (WGM shift/time) decreased noticeably for the first step (adsorption of ADC), which is an indication of slower adsorption at a lower mass concentration. The behavior is probably related to the aforementioned differences between PAH and ADC.

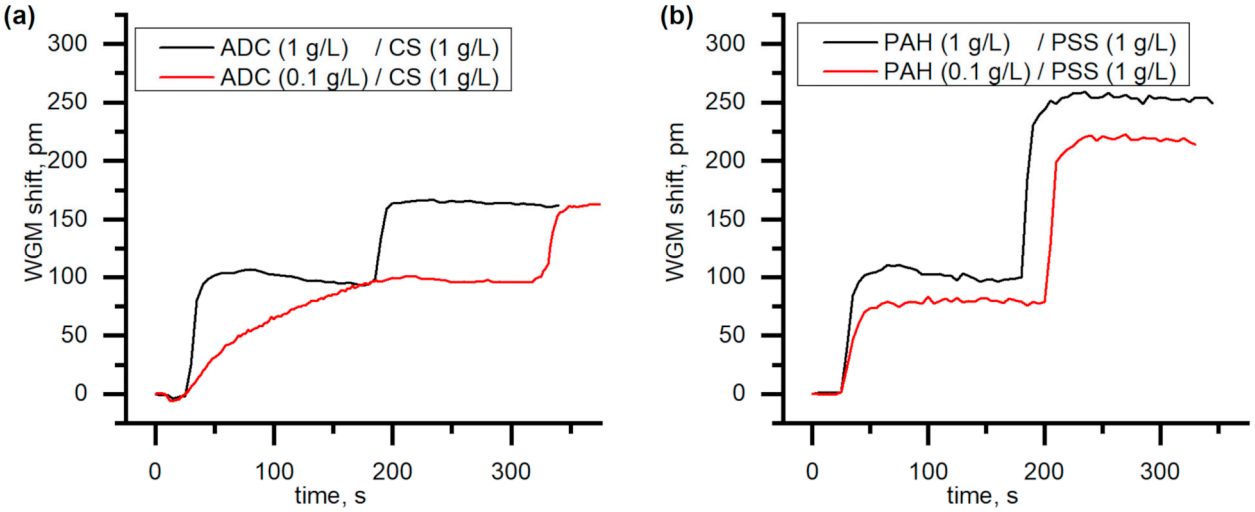


Figure 2. Results of whispering gallery mode adsorption experiments for the layer-by-layer assembling of a bilayer of (**a**) aminoethylamino-6-deoxy cellulose/ADC and cellulose sulfate/CS or (**b**) poly(allylamine)/PAH and poly(styrene sulfonate)/PSS with two different mass concentrations for the polycation (black: 1 g/L, red: 0.1 g/L) zoomed in for the third bilayer adsorption (after normalization to t = 0 s and WGM shift = 0 pm).

The LbL-coating process was furthermore investigated with respect to the zeta-potential at the surface (Figure 3). For this purpose, poly(styrene) particles were precoated with two double layers of PSS and PAH and the change in zeta-potential was monitored for the following adsorption steps with the three different polyelectrolyte combinations. As a general trend, the values alternated between positive values from about 5 to 30 mV (if the outer layer was a polycation) and negative values of about −35 to −40 mV (if the outer layer was a polyanion), which was the expected behavior. Only in the case of the first and last layer was a slightly larger charge reversal observed for PAH/PSS in comparison to the polysaccharide-based polyelectrolytes. This finding was surprising considering the lower charge density of the polysaccharide-based polycations and the slightly weaker interactions in their LbL-assemblies. The reason for this finding is not fully clear yet.

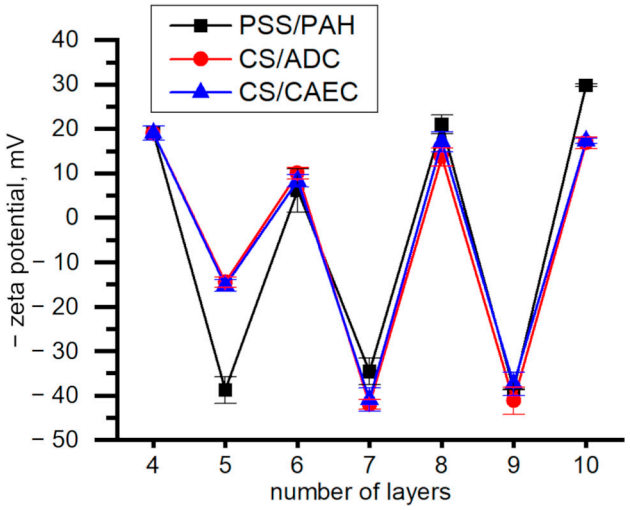


Figure 3. Zeta-potential (measured in pH 7 buffer) of polystyrene particles that were precoated with two double layers of poly(styrene sulfonate)/PSS and poly(allylamine)/PAH followed by alternating layers of polyanions (PSS; CS: cellulose sulfate) and polycations (PAH; ADC: aminoethylamino-6-deoxy cellulose; CAEC: cellulose (2-(ethylamino)ethyl)carbamate).

The experiments have demonstrated that polysaccharide-based LbL-layers can be assembled in a similar manner to materials derived from synthetic polyelectrolytes. The stability at high pH values is lower but these might not be relevant for physiological conditions or can also be exploited for deliberate disassembly. Moreover, biobased polysaccharide materials have inherent advantages in the context of biomedical applications [28,29,34,35]. The facile LbL-deposition process and the distinct reversal of the surface zeta-potential make the polysaccharide derivatives suitable candidates for the preparation of microcapsules and the encapsulation of drug compounds [9]. Thus, it was studied if polysaccharide-based capsules can be prepared by the LbL-assembling process. For this purpose, two types of µm-sized silica particles were used as templates: (i) non-porous particles and (ii) porous particles that were additionally loaded with proteins. Subsequently, the templates were dissolved by treatment with ammonium hydrogen difluoride to obtain the desired capsules [41].

Due to the negative zeta-potential of silica, adsorption was initiated by adsorbing one layer of polycation (PAH, ADC, CAEC) first followed by three bilayers of alternating polyanion (PSS, CS) and polycation (PAH, ADC, CAEC). Final, one layer of polyanion (PSS, CS) was deposited during the silica core removal step. The combination of ADC and CS aggregated during the experiments and no coated individual particles were obtained. The reason might be the strong exponential growth of ADC adsorption that was observed during the WGM experiments. These have shown that, at the third bilayer, the adsorbed mass is almost double the amount compared to PAH, which can result in the formation of a large and highly viscous coating on the surface and ultimately aggregation of the particles. For PAH/PSS and CAEC/CS, it was possible to coat silica template particles without aggregation. Subsequently, the coated particles were treated with ammonium hydrogen difluoride, which is able to penetrate the LbL-layers due to its low molecular weight and dissolve the solid silica core. For visualization, the CAEC/CS assemblies were treated with 4-chloro-7-nitrobenzo-2-oxa-1,3-diazole (NBD-Cl), which binds to free amino-groups and creates a strong fluorescence (Figure 4). The confocal laser scanning microscopy (CLSM) images clearly showed a distinct spherical layer instead of a uniform distribution of the NBD dye, i.e., the formation of an outer LbL-layer can be confirmed. Furthermore, drying of the assemblies resulted in a collapse of the structure, which clearly indicated that the silica core was removed and that the LbL-capsules were successfully obtained.

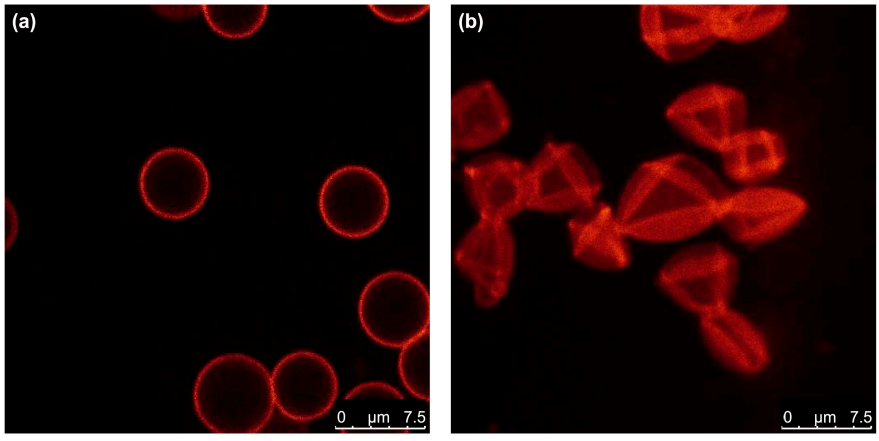


Figure 4. Confocal laser scanning microscopy images capsules obtained by layer-by-layer assembling of cellulose (2-(ethylamino)ethyl)carbamate and cellulose sulfate that were functionalized at the amino groups with fluorescent 4-chloro-7-nitrobenzo-2-oxa-1,3-diazole (**a**) before and (**b**) after drying. Settings: 64× objective, 5× zoom, excitation at 405 nm, intensity of 15 %, emission from 450 to 600 nm, photomultiplier at 800 V.

The intention of this work was to develop polysaccharide-based LbL-assemblies that can be employed for biomedical applications such as drug encapsulation and delivery as alternatives to synthetic polymer capsules. To evaluate the permeability of the different

LbL-layers, two anionic dye probes were employed: sulfo-rhodamine (sRho) as a low-molecular compound (559 g/mol) and dye-labeled Rho-PSS as a high-molecular compound (70 kDa). The probes were applied to the exterior of the capsules at different pH values and CLSM images were recorded to evaluate if the dyes can penetrate the capsule wall (Figure 5). For PAH/PSS capsules, it was observed that the whole capsules were filled with the fluorescent sRho at both investigated pH values of 7 and 8 whereas no dye loading was observed for PSS-Rho. Thus, it can be concluded that the PAH/PSS capsules are permeable for small molecules but not for polymeric compounds, which is in good agreement with previous literature data [9]. For the polysaccharide-based CAEC/CS capsules, it was found that the LbL-layer is permeable for sRho at a pH value of 7. Within 15 min, the low-molecular dye entered the capsules and filled up the void. No penetration occurred for the high-molecular PSS-Rho. Surprisingly, the CAEC/CS capsules were impenetrable for sRho when the dye was applied at a slightly higher pH value of 8. This means that it is possible to switch the permeability of the polysaccharide-based capsules around physiological conditions, which is of great interest for the encapsulation and delivery of low-molecular drugs. Permeability changes in LbL-capsules in response to changes in temperature, pH value, and ionic strength have been reported previously for synthetic polymer systems but they are relatively new for polysaccharide-based assemblies [43,44]. The mechanism behind the pH-responsiveness of the polysaccharide-based capsules is not clear yet but it can be speculated that it is caused by a partial deprotonation of CAEC.

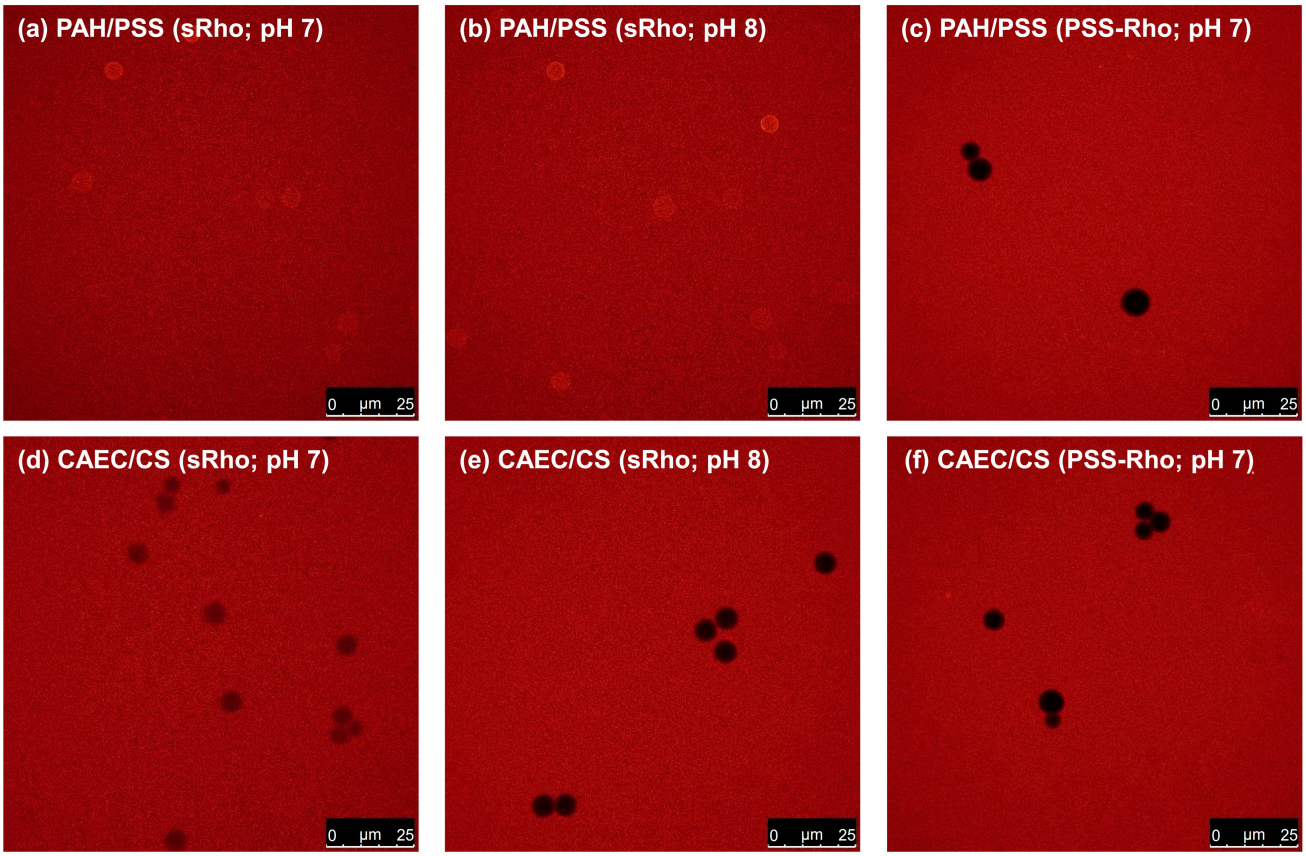


Figure 5. Confocal laser scanning microscopy images of capsules obtained by layer-by-layer assembling of polycations (PAH: poly(allylamine); CAEC: cellulose (2-(ethylamino)ethyl)carbamate and polyanions (PSS: poly(styrene sulfonate); CS: cellulose sulfate)) that were incubated with low-molecular sulfo-rhodamine (sRho) or high-molecular Rho-labeled PSS (PSS-Rho; 70 kDA) at different pH values. Settings: 63× objective, 1.5× zoom, excitation at 532 nm, intensity of 33 %, emission from 545 to 625 nm, photomultiplier at 650 V (**a**,**b**,**e**,**f**) or 685 V (**c**,**d**).

The experiments have shown that small molecules can permeate into polysaccharide-based LbL-capsules prepared by using silica particle templates whereas large molecules cannot penetrate the capsule layer. Thus, the process was adopted to encapsulate macromolecular compounds as a potential drug delivery approach. As a proof of concept, porous silica particles were employed as templates and loaded with two model proteins, namely streptavidin (Mw 60 kDa) and ovomucoid (Mw 28 kDa). The proteins were previously labeled with Rho for better visualization. Afterwards, the protein-loaded particles were covered with three LbL-bilayers of CS/CAEC and the silica core was dissolved by treatment with ammonium hydrogen difluoride while applying the final layer of CS. As can be deduced from the CLSM images, the porous particles took up a high amount of the labeled proteins, which did not get lost during the further processes of LbL-encapsulation and core dissolution (Figures 6 and 7). Despite the loading with proteins, removal of the silica core was feasible as evidence by CLSM images of dried capsules (Figure 6). These showed (a) that the structure collapsed and (b) that the dye-labeled proteins were encapsulated. Contrary to the empty capsules described above, the protein-loaded capsules showed a more disc-like form, which suggests that they were filled with the high-molecular proteins (compare Figures 4b and 6b).

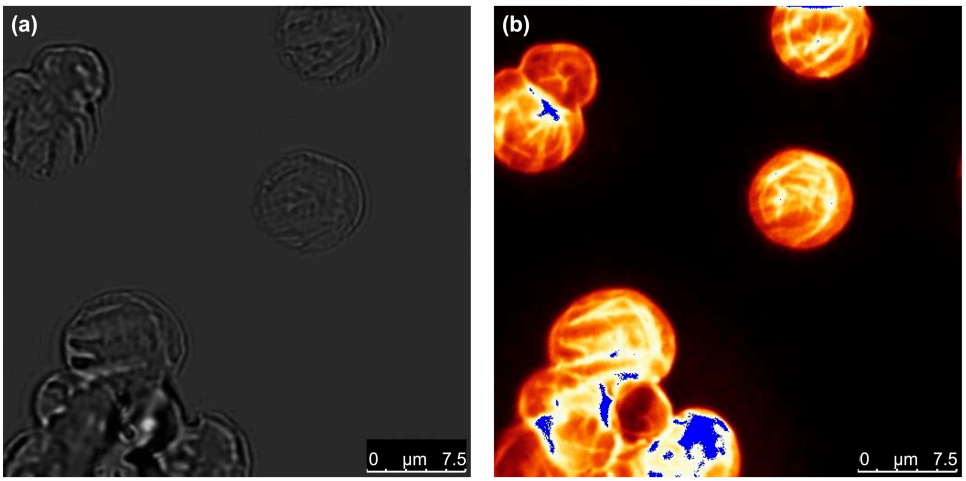


Figure 6. Confocal laser scanning microscopy images in transmission (**a**) and fluorescence mode (**b**) of capsules obtained by layer-by-layer assembling of cellulose (2-(ethylamino)ethyl)carbamate and cellulose sulfate after loading with rhodamine-labeled streptavidin and drying. Settings 63× objective, 1× zoom, excitation at 532 nm, intensity of 33 %, emission from 545 to 625 nm, photomultiplier at 750 V.

The protein-loaded LbL-capsules were characterized further by CLSM experiments in the non-dried state (Figure 7). Images were taken directly after the final capsule preparation step (0 days) and after storage of the capsules in buffered aqueous solution (pH value of 7.4) for 4 days. The initial images showed strong fluorescence of the capsules, indicating that the dye-labeled proteins were entrapped within the capsules and not destroyed by treatment with ammonium hydrogen difluoride. Moreover, the capsules still showed strong fluorescence after storage. The average fluorescence intensity (in gray values) was quantified over at least 15 CAE/CS capsules. A calibration with dye-labeled protein solutions of known concentration was performed to quantify the amount of encapsulated proteins. For streptavidin–Rho, fluorescence intensities of 122 ± 35 gray values (0 days) and 123 ± 24 gray values (days) were determined, which correspond to a mass concentration for the protein within the capsules of 73 g/L. Similar values were observed for the encapsulation of ovomucoid–Rho, with fluorescence intensities of 95 ± 13 gray values (0 days) and 93 ± 30 gray values (days) and a protein mass concentration of 76 g/L. The results clearly demonstrate that proteins were successfully encapsulated by the LbL-approach.

Furthermore, the capsules showed no leaking or disintegration over time that would result in an undesired release.

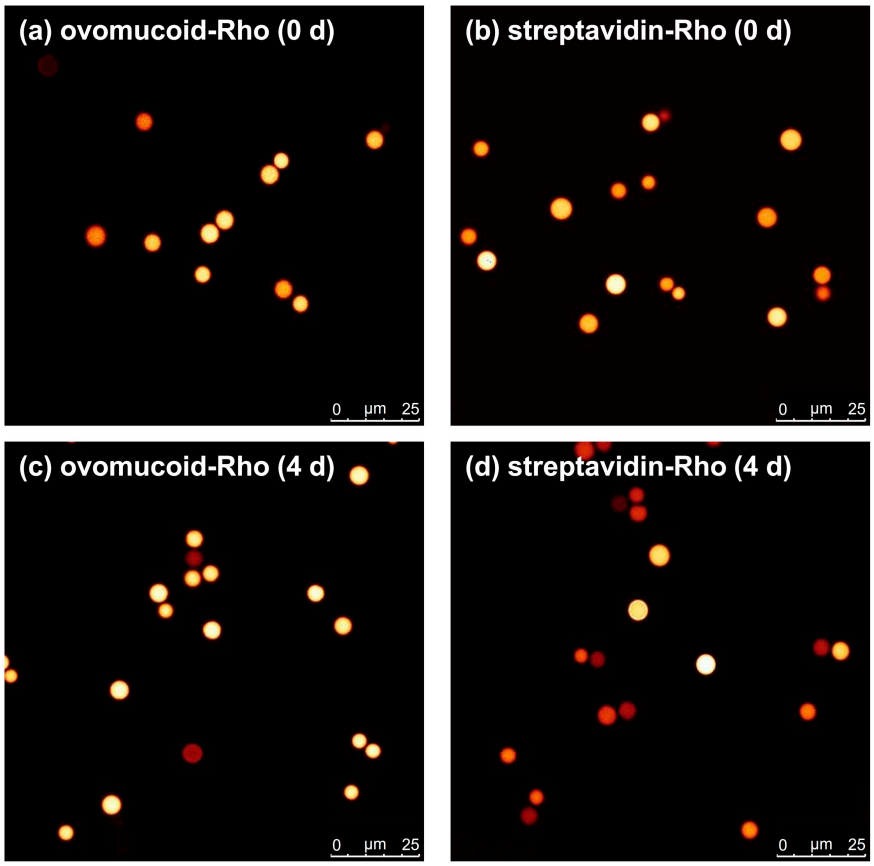


Figure 7. Confocal laser scanning microscopy images of capsules obtained by layer-by-layer assembling of cellulose (2-(ethylamino)ethyl)carbamate and cellulose sulfate that were loaded with rhodamine-labeled (Rho) streptavidin or ovomucoid and incubated in PBS-buffer for up to 4 days. Settings: 63× objective, 1× zoom, excitation at 532 nm, intensity of 33 %, emission from 545 to 625 nm, photomultiplier at 500 V.

4. Conclusions

The layer-by-layer (LbL) assembling of polysaccharide-based polyelectrolytes, namely polycationic aminoethylamino-6-deoxy cellulose (ADC) and cellulose (2-(ethylamino)ethyl) carbamate (CAEC), as well as polyanionic cellulose sulfate (CS) was studied in this work. The kinetics of the stepwise adsorption as well as the stability of the bilayers were evaluated by whispering gallery mode (WGM) experiments. Similar zeta-potential values were determined for all LbL-assemblies (5 to 30 mV for cationic surfaces and around −40 mV for anionic surfaces) but differences in adsorbed masses were observed. While synthetic polymers showed a classical linear increase for the LbL-layers, an explicit exponential growth regime was observed for polysaccharide-based LbL-assemblies. It can be postulated that the polysaccharide-based LbL-materials will exhibit broad applicability in biomedical areas (e.g., surface coating, bioencapsulation, drug delivery) due to the reported biocompatibility and biodegradability of the starting polymers. It was demonstrated in a proof of concept that proteins can be entrapped within the developed polysaccharide-based LbL-capsules (up to protein mass concentrations of around 70 g/L inside the capsules). Preliminary results showed that the proteins retain their bioactivity, which is currently studied in detail in a comprehensive work. Moreover, it was shown that the permeability of polysaccharide-based LbL-membranes is pH-responsive and can be switched to potentially release drugs under physiological conditions. This behavior that was not observed for the synthetic polymer LbL-assemblies is currently under comprehensive investigation.

Author Contributions: Conceptualization, S.W., L.D. and T.H.; methodology, S.W. and L.D.; formal analysis, S.W., M.O. and A.D.; investigation, S.W., M.O. and A.D.; data curation, S.W., M.O. and A.D.; writing—original draft preparation, S.W., M.G. and L.D.; writing—review and editing, S.W., T.H., M.G. and L.D.; funding acquisition, M.G. and T.H. All authors have read and agreed to the published version of the manuscript.

Funding: This research was partly funded by the German Federal Ministry of Food and Agriculture, based on an enactment of the German Bundestag, grant number 2220NR252X.

Data Availability Statement: The original contributions presented in the study are included in the article; further inquiries can be directed to the corresponding authors.

Conflicts of Interest: S. Wagner, M. Olszyna, A. Domac, and L. Dähne were employed by the company Surflay GmbH. Aside from that, they and all other authors declare that the research was conducted in the absence of any commercial or financial relationships that could be constructed as potential conflicts of interest.

References

1. Decher, G.; Schlenoff, J.B. *Multilayer Thin Films: Sequential Assembly of Nanocomposite Materials*; Wiley-VCH Verlag GmbH & Co. KGaA: Weinheim, Germany, 2012.
2. Decher, G.; Hong, J.-D. Buildup of Ultrathin Multilayer Films by a Self-assembly Process, 1 Consecutive Adsorption of Anionic and Cationic Bipolar Amphiphiles on Charged Surfaces. *Makromol. Chem. Macromol. Symp.* **1991**, *46*, 321–327. [CrossRef]
3. Decher, G.; Eckle, M.; Schmitt, J.; Struth, B. Layer-by-Layer Assembled Multicomposite Films. *Curr. Opin. Colloid Interface Sci.* **1998**, *3*, 32–39. [CrossRef]
4. Gao, C.; Leporatti, S.; Donath, E.; Möhwald, H. Surface Texture of Poly(styrenesulfonate sodium salt) and Poly(diallyldimethylammonium chloride) Micron-Sized Multilayer Capsules: A Scanning Force and Confocal Microscopy Study. *J. Phys. Chem. B* **2000**, *104*, 7144–7149. [CrossRef]
5. Leporatti, S.; Voigt, A.; Mitlöhner, R.; Sukhorukov, G.; Donath, E.; Möhwald, H. Scanning Force Microscopy Investigation of Polyelectrolyte Nano- and Microcapsule Wall Texture. *Langmuir* **2000**, *16*, 4059–4063. [CrossRef]
6. Donath, E.; Sukhorukov, G.B.; Caruso, F.; Davis, S.A.; Möhwald, H. Novel Hollow Polymer Shells by Colloid-Templated Assembly of Polyelectrolytes. *Angew. Chem. Int. Ed.* **1998**, *37*, 2201–2205. [CrossRef]
7. Díez-Pascual, A.M.; Rahdar, A. LbL Nano-Assemblies: A Versatile Tool for Biomedical and Healthcare Applications. *Nanomaterials* **2022**, *12*, 949. [CrossRef]
8. Zhang, S.; Xia, F.; Demoustier-Champagne, S.; Jonas, A.M. Layer-by-Layer Assembly in Nanochannels: Assembly Mechanism and Applications. *Nanoscale* **2021**, *13*, 7471–7497. [CrossRef]
9. Peyratout, C.S.; Dähne, L. Tailor-Made Polyelectrolyte Microcapsules: From Multilayers to Smart Containers. *Angew. Chem. Int. Ed.* **2004**, *43*, 3762–3783. [CrossRef]
10. Zhao, S.; Caruso, F.; Dähne, L.; Decher, G.; De Geest, B.G.; Fan, J.; Feliu, N.; Gogotsi, Y.; Hammond, P.T.; Hersam, M.C.; et al. The Future of Layer-by-Layer Assembly: A Tribute to ACS Nano Associate. *ACS Nano* **2019**, *13*, 6151–6169. [CrossRef]
11. Gericke, M.; Amaral, A.J.R.; Budtova, T.; De Wever, P.; Groth, T.; Heinze, T.; Höfte, H.; Huber, A.; Ikkala, O.; Kapuśniak, J.; et al. The European Polysaccharide Network of Excellence (EPNOE) Research Roadmap 2040: Advanced Strategies for Exploiting the Vast Potential of Polysaccharides as Renewable Bioresources. *Carbohydr. Polym.* **2024**, *326*, 121633. [CrossRef]
12. Delvart, A.; Moreau, C.; Cathala, B. Dextrans and Dextran Derivatives as Polyelectrolytes in Layer-by-Layer Processing Materials—A Review. *Carbohydr. Polym.* **2022**, *293*, 119700. [CrossRef] [PubMed]
13. Hu, B.; Guo, Y.; Li, H.; Liu, X.; Fu, Y.; Ding, F. Recent Advances in Chitosan-based Layer-by-Layer Biomaterials and Their Biomedical Applications. *Carbohydr. Polym.* **2021**, *271*, 118427. [CrossRef] [PubMed]
14. de Alvarenga, E.S.; Pereira de Oliveira, C.; Roberto Bellato, C. An Approach to Understanding the Deacetylation Degree of Chitosan. *Carbohydr. Polym.* **2010**, *80*, 1155–1160. [CrossRef]
15. Kou, S.; Peters, L.M.; Mucalo, M.R. Chitosan: A Review of Sources and Preparation Methods. *Int. J. Biol. Macromol.* **2021**, *169*, 85–94. [CrossRef] [PubMed]
16. Wang, Q.Z.; Chen, X.G.; Liu, N.; Wang, S.X.; Liu, C.S.; Meng, X.H.; Liu, C.G. Protonation Constants of Chitosan with Different Molecular Weight and Degree of Deacetylation. *Carbohydr. Polym.* **2006**, *65*, 194–201. [CrossRef]
17. Lundin, M.; Solaqa, F.; Thormann, E.; Macakova, L.; Blomberg, E. Layer-by-Layer Assemblies of Chitosan and Heparin: Effect of Solution Ionic Strength and pH. *Langmuir* **2011**, *27*, 7537–7548. [CrossRef] [PubMed]
18. Martins, G.V.; Mano, J.F.; Alves, N.M. Nanostructured Self-Assembled Films Containing Chitosan Fabricated at Neutral pH. *Carbohydr. Polym.* **2010**, *80*, 570–573. [CrossRef]
19. Such, G.K.; Johnston, A.P.R.; Caruso, F. Layer-by-Layer Assembled Capsules for Biomedical Applications. In *Comprehensive Nanoscience and Technology*; Andrews, D.L., Scholes, G.D., Wiederrecht, G.P., Eds.; Academic Press: Amsterdam, The Netherlands; Cambridge, MA, USA, 2011; pp. 359–377.

20. Tong, W.; Song, X.; Gao, C. Layer-by-Layer Assembly of Microcapsules and Their Biomedical Applications. *Chem. Soc. Rev.* **2012**, *41*, 6103–6124. [CrossRef] [PubMed]
21. Campbell, J.; Abnett, J.; Kastania, G.; Volodkin, D.; Vikulina, A.S. Which Biopolymers Are Better for the Fabrication of Multilayer Capsules? A Comparative Study Using Vaterite $CaCO_3$ as Templates. *ACS Appl. Mater. Interfaces* **2021**, *13*, 3259–3269. [CrossRef]
22. Li, W.; Lei, X.; Feng, H.; Li, B.; Kong, J.; Xing, M. Layer-by-Layer Cell Encapsulation for Drug Delivery: The History, Technique Basis, and Applications. *Pharmaceutics* **2022**, *14*, 297. [CrossRef]
23. Hileuskaya, A.; Ihnatsyeu-Kachan, A.; Kraskouski, A.; Salamianski, A.; Nikalaichuk, V.; Hileuskaya, K.; Kim, S. LbL films and Microcapsules Based on Protamine and Pectin-Ag Nanocomposite. *Mater. Today Proc.* **2022**, *54*, 28–34. [CrossRef]
24. Redolfi Riva, E.; D'Alessio, A.; Micera, S. Polysaccharide Layer-by-Layer Coating for Polyimide-Based Neural Interfaces. *Micromachines* **2022**, *13*, 692. [CrossRef] [PubMed]
25. Criado-Gonzalez, M.; Mijangos, C.; Hernández, R. Polyelectrolyte Multilayer Films Based on Natural Polymers: From Fundamentals to Bio-Applications. *Polymers* **2021**, *13*, 2254. [CrossRef] [PubMed]
26. Ganjeh, A.M.; Saraiva, J.A.; Pinto, C.A.; Casal, S.; Gonçalves, I. Recent Advances in Nano-reinforced Food Packaging Based on Biodegradable Polymers Using Layer-by-Layer Assembly: A Review. *Carbohydr. Polym. Technol. Appl.* **2024**, *7*, 100395. [CrossRef]
27. Heinze, T.; Elschner, T.; Ganske, K. Aminocelluloses—Polymers with Fascinating Properties and Application Potential. In *Cellulose Science and Technology*; John Wiley & Sons, Inc.: Hoboken, NJ, USA, 2018; pp. 1–28.
28. Finger, S.; Zieger, M.; Wiegand, C.; Liebert, T.; Heinze, T.; Elsner, P.; Hipler, U.-C. Biocompatibility and Antibacterial Effects of 6-Deoxy-6-Aminoethyleneamino Cellulose. *J. Biosci. Med.* **2018**, *6*, 51–62. [CrossRef]
29. Ganske, K.; Wiegand, C.; Hipler, U.-C.; Heinze, T. Synthesis of Novel Cellulose Carbamates Possessing Terminal Amino Groups and Their Bioactivity. *Macromol. Biosci.* **2016**, *16*, 451–461. [CrossRef] [PubMed]
30. Heinze, T.; Pfeifer, A.; Koschella, A.; Schaller, J.; Meister, F. Solvent-free Synthesis of 6-Deoxy-6-(ω-aminoalkyl)amino cellulose. *J. Appl. Polym. Sci.* **2016**, *133*, 43987. [CrossRef]
31. Gabriel, L.; Gericke, M.; Heinze, T. Modular Synthesis of Non-charged and Ionic Xylan Carbamate Derivatives from Xylan Carbonates. *Carbohydr. Polym.* **2019**, *207*, 782–790. [CrossRef] [PubMed]
32. Gericke, M.; Atmani, Z.; Skodda, L.H.; Heinze, T. Synthesis and Characterization of Polysaccharide Carbamates and Mixed Carbamates with Tunable Water Solubility. *Carbohydr. Polym. Technol. Appl.* **2024**, *7*, 100479. [CrossRef]
33. Gericke, M.; Doliška, A.; Stana, J.; Liebert, T.; Heinze, T.; Stana-Kleinschek, K. Semi-Synthetic Polysaccharide Sulfates as Anticoagulant Coatings for PET, 1—Cellulose Sulfate. *Macromol. Biosci.* **2011**, *11*, 549–556. [CrossRef]
34. Zeng, K.; Doberenz, F.; Lu, Y.-T.; Nong, J.P.; Fischer, S.; Groth, T.; Zhang, K. Synthesis of Thermoresponsive PNIPAM-Grafted Cellulose Sulfates for Bioactive Multilayers via Layer-by-Layer Technique. *ACS Appl. Mater. Interfaces* **2022**, *14*, 48384–48396. [CrossRef] [PubMed]
35. Strätz, J.; Liedmann, A.; Heinze, T.; Fischer, S.; Groth, T. Effect of Sulfation Route and Subsequent Oxidation on Derivatization Degree and Biocompatibility of Cellulose Sulfates. *Macromol. Biosci.* **2020**, *20*, 1900403. [CrossRef] [PubMed]
36. Panda, P.K.; Yang, J.-M.; Chang, Y.-H. Preparation and Characterization of Ferulic Acid-modified Water Soluble Chitosan and Poly (γ-glutamic acid) Polyelectrolyte Films Through Layer-by-Layer Assembly Towards Protein Adsorption. *Int. J. Biol. Macromol.* **2021**, *171*, 457–464. [CrossRef] [PubMed]
37. Livanovich, K.S.; Sharamet, A.A.; Shimko, A.N.; Shutava, T.G. Layer-by-Layer Films of Polysaccharides Modified with Poly(*N*-vinylpyrrolidone) and Poly(vinyl alcohol). *Heliyon* **2021**, *7*, e08224. [CrossRef] [PubMed]
38. Monteiro, L.P.G.; Borges, J.; Rodrigues, J.M.M.; Mano, J.F. Unveiling the Assembly of Neutral Marine Polysaccharides into Electrostatic-Driven Layer-by-Layer Bioassemblies by Chemical Functionalization. *Mar. Drugs* **2023**, *21*, 92. [CrossRef] [PubMed]
39. Heinze, T.; Nikolajski, M.; Daus, S.; Besong, T.M.D.; Michaelis, N.; Berlin, P.; Morris, G.A.; Rowe, A.J.; Harding, S.E. Protein-like Oligomerization of Carbohydrates. *Angew. Chem. Int. Ed.* **2011**, *50*, 8602–8604. [CrossRef] [PubMed]
40. Himmelhaus, M.; Krishnamoorthy, S.; Francois, A. Optical Sensors Based on Whispering Gallery Modes in Fluorescent Microbeads: Response to Specific Interactions. *Sensors* **2010**, *10*, 6257–6274. [CrossRef] [PubMed]
41. Dähne, L.; Baude, B. Process for the Preparation of CS Particles and Microcapsules Using Porous Templates as well as CS Particles and Microcapsules. Patent DE102004013637A1, 19 March 2004.
42. Elżbieciak-Wodka, M.; Kolasińska-Sojka, M.; Nowak, P.; Warszyński, P. Comparison of Permeability of Poly(allylamine hydrochloride)/and Poly(diallyldimethylammonium chloride)/poly(4-styrenesulfonate) Multilayer films: Linear vs. Exponential Growth. *J. Electroanal. Chem.* **2015**, *738*, 195–202. [CrossRef]
43. Gao, C.; Leporatti, S.; Moya, S.; Donath, E.; Möhwald, H. Swelling and Shrinking of Polyelectrolyte Microcapsules in Response to Changes in Temperature and Ionic Strength. *Chem.—A Eur. J.* **2003**, *9*, 915–920. [CrossRef]
44. Antipov, A.A.; Sukhorukov, G.B.; Leporatti, S.; Radtchenko, I.L.; Donath, E.; Möhwald, H. Polyelectrolyte Multilayer Capsule Permeability Control. *Colloids Surf. A Physicochem. Eng. Asp.* **2002**, *198–200*, 535–541. [CrossRef]

Disclaimer/Publisher's Note: The statements, opinions and data contained in all publications are solely those of the individual author(s) and contributor(s) and not of MDPI and/or the editor(s). MDPI and/or the editor(s) disclaim responsibility for any injury to people or property resulting from any ideas, methods, instructions or products referred to in the content.